PCCP

Glycerol condensed phases

Part II.† A molecular dynamics study of the conformational structure and hydrogen bonding

Riccardo Chelli,[ab] Piero Procacci,[ab] Gianni Cardini[ab] and Salvatore Califano*[ab]

[a] *Laboratorio di Spettroscopia Molecolare, Dipartimento di Chimica, Via Gino Capponi 9, 50121 Firenze, Italy*
[b] *European Laboratory for Nonlinear Spectroscopy (LENS), Largo E. Fermi 2, 50125 Florence, Italy*

Received 17th November 1998, Accepted 6th January 1999

An analysis of the conformational properties and hydrogen bonding in the condensed phases of glycerol is reported using the same model as adopted in Part I (*Phys. Chem. Chem. Phys.*, 1999, **1**, 871). Structural properties of the liquid and glassy states are analyzed in relation to the molecular backbone conformation of the glycerol molecule. The effects of hydrogen bonding and of temperature on the conformational distribution are analyzed. The structural and dynamical properties of hydrogen bonding in glycerol are also investigated. The results are consistent with available experimental observations and clarify many important and interrelated aspects of the microscopic structure of liquid, glassy and crystalline phases of glycerol.

1 Introduction

In Part I (ref. 1) we have presented a molecular dynamics (MD) simulation of the static and dynamic properties of glycerol in the crystal, glass and liquid phases. With the aid of a suitable potential model, we have computed several properties of the condensed phases as a function of temperature, including the static structure factor, the molar volume, the density of vibrational states, the mean square displacements of the atoms and the specific heat. The calculated quantities gave an excellent agreement with experimental data from incoherent neutron diffraction and calorimetric experiments.

In the present paper we report an extension of the previous MD simulation aimed at understanding the structure of the H-bond network and the interplay of intra- and intermolecular interactions on the equilibrium conformational distribution in the condensed phases of glycerol. We show that the conformational distribution has a significant role in determining the properties of the super-cooled liquid and in driving the glass transition.

Glycerol is a highly flexible molecule forming both intra- and inter-molecular hydrogen bonds. Liquid glycerol exhibits an anomalous temperature behaviour of the viscosity coefficient[2,3] and of dielectric relaxation times[4,5] due to the existence of an extended H-bond network.[4,6–8] Glycerol easily forms a super-cooled liquid which, by lowering the temperature, undergoes, at about 187 K, a transition to a glassy state[9] whose nature has been the object of several investigations.[9–14] Crystallization, occurring at 291 K,[15] cannot be directly reached from the liquid but requires special procedures.[16,17]

The conformational space of the glycerol molecule is quite complex: six types of backbone conformers exist, classified in the literature on the subject, according to the dihedral angles involving the two CCCO torsions. Each backbone conformer may in turn exhibit different preferential arrangements of the hydroxy hydrogens.

† Part I, ref. 1.

Early electron diffraction studies on the liquid state[18] suggested the presence of mainly unfolded conformers of αα and αγ type (for the notation of the conformers see Fig. 1 and section 2). The αα backbone conformation, typical of crystalline glycerol,[16] was also invoked in neutron scattering studies[6,7] to explain the observed structure factors at large wave vectors. However, in a recent neutron scattering investigation of the glassy state,[19] a preferential unfolded conformational structure of the βγ type has been proposed for the best fit of the experimental structure factor. Diffraction studies provide valuable information on the structural properties of the condensed phases but the subtle details of the conformational structures are usually inferred by fitting procedures based on a weakly selective function such as the structure factor at large wave vectors. Hence, computer simulations using a realistic atomistic model of glycerol can give valuable insights into the microscopic details of the structure of the condensed phases. Early MD studies by Root and Stillinger[20]

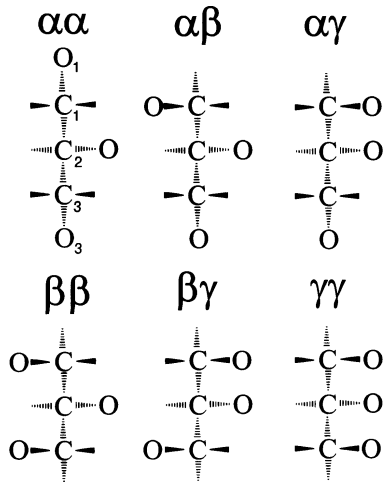

Fig. 1 Backbone conformers of the glycerol molecule. Prochiral partners (see text) for αβ, βγ and αγ are not displayed.

focused on the structure of the liquid but the significance of the results was limited by the small size of the samples (32 molecules) and by the short simulation time of less than 1 ps. More recently Root and Berne[21] studied the effect of pressure on H-bond interactions in liquid glycerol. In general, however, little attention to the problem of the conformational structure of glycerol has been given by past MD studies.

In this paper we present a thorough analysis of the structural and dynamical properties of the liquid and glass phases in a wide temperature range, using a MD simulation. The potential model proposed in Part I,[1] which reproduces very satisfactorily the structural and dynamical properties of glycerol in the condensed phases, has been adopted. The data obtained in the present computer simulations are consistent with all available experimental observations and clarify many important and interrelated aspects of the microscopic structure of liquid, glassy and crystalline glycerol.

The paper is organized as follows. In section 2 the conformational phase space of the glycerol molecule and its energetics are described; in addition the role of the intra- and inter-molecular interactions in determining the equilibrium conformational distribution in different phases, as a function of temperature, are discussed. In section 3 the microscopic structure of the liquid and glass are analyzed, focusing on the role and importance of H-bonding.

2 The conformational space of glycerol

In the glycerol molecule all bonds are single and hence there is considerable freedom of internal rotations. The traditional classification of the various molecular structures[18] is based on the concept of *backbone* conformer, defined by the structure of the heavy atom skeleton irrespective of the positions of the hydrogen atoms. The backbone structure can be unambiguously identified by assigning the two dihedral angles $O_1C_1C_2C_3$ and $C_1C_2C_3O_3$ involving the three carbon atoms and the terminal oxygens (see Fig. 1). Choosing the dihedral angle of the *trans* conformation as the zero with *positive* clockwise rotation around the vectors C_1C_2 and C_2C_3, we classify the dihedral angular ranges $-60° < \theta < 60°$, $60° < \theta < 180°$ and $180° < \theta < 300°$ as α, β and γ, respectively.[18] Since there are two dihedral angles, six possible backbone conformers can be identified as shown in Fig. 1. For example, in the αα conformer both dihedral angles are in the $-60° < \theta < 60°$ range. Glycerol is a molecule with no asymmetric carbons. However, because of its property to be asymmetrically metabolized,[22–26] glycerol is frequently defined as *prochiral*.[27] From this point of view a backbone conformer of the χζ kind (the symbols χ, ζ refer to the entire angular *range*, while the symbols θ,ϕ indicate a *specific value* of the angle), with $\chi \neq \zeta$, has a backbone prochiral counterpart in ζχ. Conformers of the χχ kind have no backbone prochiral partners. The conformational space is further complicated by the presence of the three OH groups. Each dihedral angle HOCC around the CO bond has several conformational possibilities and therefore, in principle, a large number of *all atoms* conformers can be defined for each backbone conformer, although most of these *all atoms* conformations are inhibited due to steric hindrance.

For a correct understanding of the microscopic properties of the condensed phases, two basic pieces of information are needed: the energy and the structure of the stable conformers and their relative abundance.

Ab initio calculations[28–30] predict αα, αγ and γγ backbone conformers as the most stable ones. To check whether our potential model gives the same results, we have generated 7500 random configurations for each different backbone conformer of glycerol molecules and minimized the structure using the conjugate gradient method.[31] The results agree with the *ab initio* calculations and confirm the stability of the αα, αγ and γγ conformers. We obtained the four αα, the seven αγ and the four γγ minimum energy structures shown in Fig. 2. Other conformers are not shown since they all have very high energies, ranging from 84 to 113 kJ mol^{-1}. The stability of the αα backbone conformer is strongly supported by the fact that it is the structure observed in the crystal.[16]

In order to answer the second question, *i.e.* the relative abundance of the different conformers, it is important to understand whether the conformations existing in the liquid and in the glass are stabilized by the inter-molecular interactions, in particular by the H-bond formation, or if their abundance is controlled essentially by the intra-molecular interactions. This is particularly necessary in the case of the γγ backbone conformer, which, despite its stability, is weakly represented in the condensed phases. We have thus performed a MD simulation in the NVT (constant particle number N, constant volume V and constant temperature T) ensemble of a sample of 1000 non-interacting molecules for 1.5 ns. We found that the running average energy for each class of conformers belonging to the same backbone conformer shows strong fluctuations due to the fact that in the limited duration of the runs the conformational space cannot be explored completely.

The lack of energy exchange in the absence of collisions is actually a strong limiting factor for a correct sampling of the conformational space. Indeed, as shown in Fig. 2, minimum configurations within the same backbone conformation differ by several kJ mol^{-1}.

A more effective method for enhancing the sampling efficiency of the conformational space is based on the principles of the umbrella sampling technique.[32] The idea is to add to the Hamiltonian an appropriate potential, U, that removes the energy barriers between conformational states and to run the MD simulation in this ensemble (indicated hereafter as the π ensemble) at constant volume and temperature. The average of any observable A, in the *canonical ensemble* with the original Hamiltonian at the same temperature T, can be recovered from the canonical averages in the π ensemble by inverse reweighting using the well known umbrella sampling formula

$$\langle A \rangle_{NVT} = \frac{\langle A e^{-U/K_B T} \rangle_\pi}{\langle e^{-U/K_B T} \rangle_\pi} \quad (1)$$

A convenient potential U is the negative of the sum of the Lennard-Jones (V_{LJ}), of the electrostatic (V_{el}) and of all HOCC torsional interactions (V_{tors}): $U = -V_{LJ} - V_{el} - V_{tors}$. This

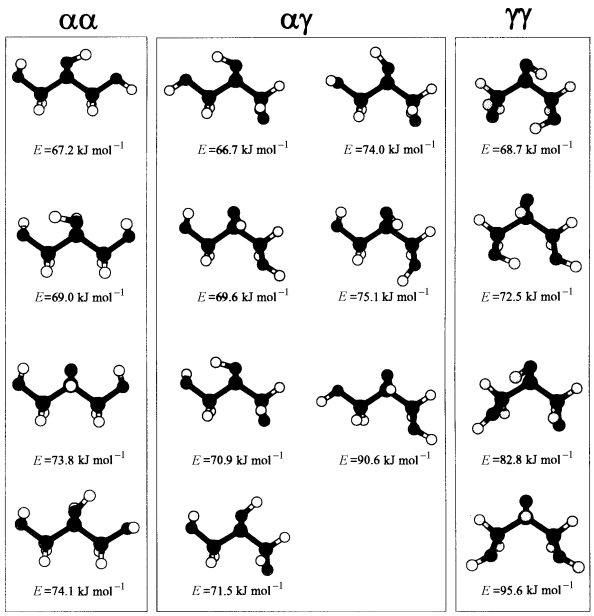

Fig. 2 Optimized structures and corresponding energies for *all atoms* conformers of αα, αγ and γγ backbone conformers.

potential clearly removes all barriers between conformational states involving torsions around the C—O bonds and strongly reduces the barriers between the backbone conformations, while leaving at the same time the distribution of bonds and bending angles close to the original canonical one.

Using eqn. (1), the probability of occurrence of a generic backbone conformation $\chi\zeta$ in the canonical NVT ensemble is given by

$$P_{\chi\zeta} = \frac{\sum_i \Omega_\chi(\theta_i)\Omega_\zeta(\phi_i)e^{-U_i/K_B T}}{\sum_i e^{-U_i/K_B T}} \quad (2)$$

where all averages are taken over the configurations in the π ensemble and the function $\Omega_\chi(\theta_i)$ is equal to one if the dihedral angle θ_i for the i-th configuration is inside the range labeled χ (with $\chi = \alpha, \beta, \gamma$) and zero otherwise. In Table 1 we report the values of $P_{\chi\zeta}$ calculated from eqn. (2) for the six conformers in the gas phase at 400 and 300 K. About 2.5×10^6 configurations, taken at regular intervals from an NVT run of 5 ns on a sample of 1000 glycerol molecules in the π ensemble, were used. $\chi\zeta$ and $\zeta\chi$ configurations must of course have equal probabilities. This condition constitutes a very severe test for the equilibrium regime. The probability of $\chi\zeta$ and $\zeta\chi$ conformations, for all the prochiral pairs, differ by less than 1%. The average energies for the backbone conformations in the gas phase at 400 and 300 K are reported in Table 2. The total energy only partially explains the observed probabilities: the Helmholtz free energy differences at, *e.g.*, 400 K, calculated on the basis of the probabilities of Table 1, are $A(\alpha\alpha) - A(\alpha\gamma) = -1.8 \pm 0.3$ kJ mol^{-1}, $A(\alpha\alpha) - A(\gamma\gamma) = -4.3 \pm 0.6$ kJ mol^{-1}, while the corresponding differences of the total energies (Table 2) are $E(\alpha\alpha) - E(\alpha\gamma) = -0.5 \pm 0.6$ kJ mol^{-1} and $E(\alpha\alpha) - E(\gamma\gamma) = -0.4 \pm 0.9$ kJ mol^{-1}. Therefore entropic effects play an important role in determining the free energy when the torsional coordinates θ and ϕ span the full conformational space.

2.1 Conformational distribution in the condensed phases

The problem of computing a reliable conformational distribution is less acute in the liquid state. Energy is in fact easily exchanged between molecules through molecular collisions and a stationary value of the conformational distribution is usually reached after a few hundreds of picoseconds irrespective of the starting configuration using conventional MD.

The effect of the inter-molecular interactions and of the temperature can be inferred by inspection of Table 1. The gas-phase distribution is only *slightly* perturbed in going to the liquid state. In the liquid, the $\alpha\alpha$ probability increases by approximately 5% at the expense of the $\gamma\gamma$ probability which decreases by the same amount. A significant increase of the $\alpha\beta$ and $\beta\alpha$ conformers occurs in the liquid, due to the fact that these conformers have an open structure and can easily form inter-molecular H-bonds. The fraction of $\alpha\gamma$ and $\gamma\alpha$ remains practically unchanged, while all other conformations, like in the gas phase, occur with negligible probability. In the glassy state, due to the lack of ergodicity, the conformational distribution is identical to that of the super-cooled liquid near the glass transition. The inter-molecular hydrogen bonds, therefore, *do not significantly stabilize* energetically unfavored gas-phase structures. In particular, the abundance of the $\beta\gamma$ conformers, recently proposed as the most probable in the glassy state,[19] remains as negligible in the liquid as in the gas phase.

We conclude therefore that the *intra-molecular* energy is the prevailing factor in determining the *average* molecular structure in the condensed phases. The effect of inter-molecular H-bond stabilization of unfolded structures, as $\alpha\alpha$ and $\alpha\gamma$, with respect to the folded $\gamma\gamma$ conformer has been invoked in the past[19,29] to explain the experimental conformational distribution. In the present study, this effect appears small compared to the intra-molecular energy effects.

The small changes with temperature in the conformational distribution are in agreement with experimental diffraction studies[6,7,19,33] where the shape of structure factors was found to be weakly dependent on the temperature and similar in the super-cooled liquid and in the glassy state. It is indeed remarkable that a steady stabilization of the $\alpha\alpha$ conformation, *i.e.*, of the molecular structure observed in the crystalline state, is observed during the cooling process from 400 K down to the super-cooled liquid and glassy state. Near the crystallization temperature ($\sim$290 K), the percentage of $\alpha\alpha$ conformers is about 50% and this fact may explain the difficulty[16,17] in obtaining crystalline glycerol given that nearly half of the molecules must undergo at least one backbone transition in the solidification process.

Table 1 Percentage probability distribution of the glycerol backbone conformations in the liquid and gas phase[a]

	400 K		300 K	
Conformer	Liquid	Gas	Liquid	Gas
$\alpha\alpha$	44 (3)	39.9 (5)	48 (1)	43.0 (8)
$\alpha\gamma + \gamma\alpha$	45 (2)	47.0 (3)	46.0 (6)	46.9 (5)
$\gamma\gamma$	6 (1)	11.0 (2)	4.4 (6)	9.8 (4)
$\alpha\beta + \beta\alpha$	3.8 (9)	1.40 (1)	1.4 (4)	0.22 (1)
$\beta\gamma + \gamma\beta$	1.2 (5)	0.67 (1)	0.2 (1)	0.11 (1)
$\beta\beta$	0.01 (1)	0.03 (1)	0	0.002 (1)

[a] Errors in the last digit are given in parentheses.

Table 2 Mean backbone conformational energies (kJ mol^{-1}) in the gas phase[a]

Conformer	400 K	300 K
$\alpha\alpha$	173.5 (4)	146.5 (4)
$\alpha\gamma$, $\gamma\alpha$	174.0 (2)	147.0 (1)
$\gamma\gamma$	173.9 (5)	148.2 (4)
$\alpha\beta$, $\beta\alpha$	190.6 (3)	163.8 (8)
$\beta\gamma$, $\gamma\beta$	192.3 (2)	166.0 (4)
$\beta\beta$	200.1 (8)	172 (2)

[a] For the $\chi\zeta$ and $\zeta\chi$ conformers (see text), the mean value is reported. The error in the last digit is given in parentheses.

2.2 Conformational dynamics

The time evolution of a generic OCCC backbone dihedral angle $\theta(t)$ has been monitored to test the ability of a given molecule to undergo conformational jumps. In the liquid phase the angular distribution of θ depends weakly on the temperature and is characterized by three approximately Gaussian distributions, peaked at about $\phi_\alpha = -5°$, $\phi_\beta = 115°$ and $\phi_\gamma = 244°$ with a half width at half maximum $\Delta\phi$ of about 16°. If $\theta(t)$ is in the angular range $\phi_i - \Delta\phi < \theta(t) < \phi_i + \Delta\phi$, a conformational jump is counted if at a later time $t + \Delta t$, $\theta(t + \Delta t)$ is found in a different angular range $\phi_j - \Delta\phi < \theta(t + \Delta t) < \phi_j + \Delta\phi$. The effective duration of a conformational transition is defined as the time needed for θ to leave the range $\phi_i - \Delta\phi < \theta < \phi_i + \Delta\phi$ to enter the different range $\phi_j - \Delta\phi < \theta < \phi_j + \Delta\phi$. The number of conformational jumps per molecule per nanosecond as a function of temperature in the liquid phase is shown in Fig. 3(a). As expected the number of jumps per molecule in the unit time increases steadily with increasing temperature. At 400 K the average lifetime for a backbone conformation is about 28 ps. The average jumping frequencies can be fitted with an Arrhenius functional form [see Fig. 3(a)]. The corresponding activation energy is estimated to be 20.2 ± 0.3 kJ mol^{-1}.

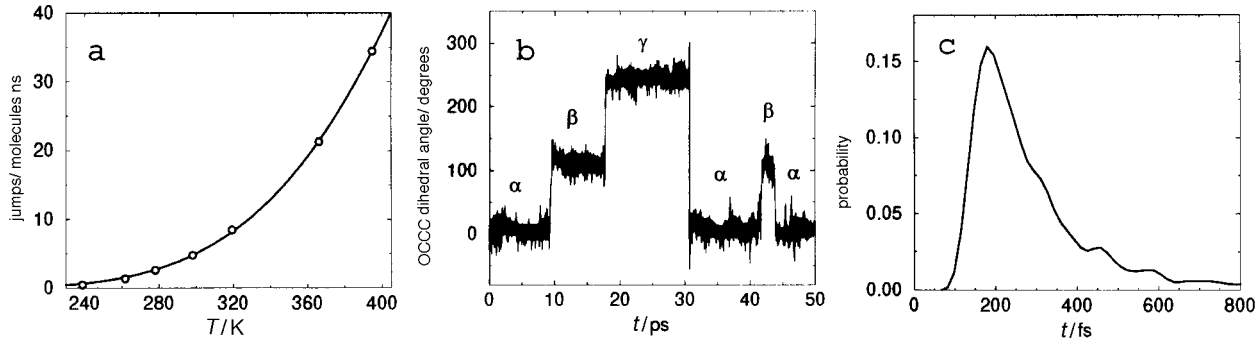

Fig. 3 (a) Average number of conformational jumps for liquid glycerol as a function of temperature. The full curve shows the fit using an Arrhenius type function. (b) Time record of the OCCC dihedral angle for a generic molecule at 400 K in glycerol. The large jump at ≈30 ps is due to a complete rotation of the CH_2OH group around the CC bond. (c) Distribution of the duration time of a conformational jump for liquid glycerol at 400 K.

The time evolution of one OCCC dihedral angle for a generic molecule in the liquid at 400 K is displayed in Fig. 3(b). Conformational jumps are very fast and occur in less than half a picosecond. The probability distribution of the duration time for conformational transitions in the liquid evaluated at 400 K are shown in Fig. 3(c). The distribution of the duration time is peaked at about 200 fs and is found to be practically independent of the temperature.

3 Hydrogen bond in the condensed phases

In a classical MD simulation the definition of inter-molecular H-bond results is in some way arbitrary due to the lack of information on the electron density. It is therefore necessary to resort to geometrical arguments for the definition of inter-molecular H-bonds. In the present paper, the H-bond is defined, according to previous papers on the subject,[21,34,35] on the basis of the O···H distance, chosen to be less than 2.45 Å (corresponding to the first minimum distance in the $g_{OH}(r)$ distribution function), and of the OH···O bond angle, chosen larger than 145°. An H-bond is assumed to be formed (destroyed) if the previously mentioned criteria are fulfilled (not fulfilled) for at least[21] 180 fs. An intra-molecular H-bond is defined in the same way, but without restriction on the OH···O bond angle.

3.1 Intra- and inter-molecular hydrogen bond

Intra-molecular H-bonds in glycerol give rise to the formation of rings with five and six atoms closed by the H-bond. Five-membered rings (H—O—C—C—O) can occur in the αα and αγ conformations, while six-membered rings (H—O—C—C—C—O) are compatible with the less abundant γγ backbone conformation. In Table 3 we show the average number of hydrogen atoms per molecule donated in inter-molecular H-bonds by some conformers in the condensed phases. The γγ conformer donates, on average, significantly less hydrogen atoms with respect to the αα, αγ and αβ, due to the stronger intra-molecular H-bond of the six-membered ring with respect to the H-bond of five-membered rings. The same behaviour is observed for the oxygen acceptors. In fact, the radial distribution functions for intra-molecular *oxygen–hydroxy hydrogen* pairs show a maximum at about 2.0 Å for γγ, while for αα and αγ this maximum is at about 2.6 Å. Since the formation of inter-molecular H-bonds requires the break of the intra-molecular ones, it is clear that αα and αγ, characterized by a less constrained structure with weaker intra-molecular H-bonds, can more easily form inter-molecular H-bonds. The relative inability of the γγ conformer to form inter-molecular H-bonds is responsible for the observed halving of its occurrence probability in going from the gas to the liquid state. As can be seen in Fig. 4, the number of intra-molecular H-bonds in the condensed phases slightly decreases as the temperature is lowered. This is a consequence of the fact that intra-molecular H-bonds are principally of five-membered ring type (αα and αγ conformers): as the temperature decreases, more and more inter-molecular H-bonds are formed at the expense of the weak intra-molecular H-bonds of the five-membered rings.

The *oxygen–hydroxy hydrogen* radial distribution function $g_{OH}(r)$ has been given in Part I (ref. 1) for different temperatures. The results are similar to those obtained in previous MD simulations[20,21] and supply clear evidence of inter-molecular H-bond formation.

The distribution of the OH···O angles is peaked at 180° with half width at half maximum of 19°, 23°, and 26° at 200, 300 and 400 K, respectively. These results are consistent with the calculations reported by Root and Berne,[21] which predict a preferential linear conformation for inter-molecular H-bonds in glycerol, and are consistent with diffraction data.[6,7,19]

Table 3 Number of hydrogen atoms per molecule involved in inter-molecular H-bonds for the backbone conformers αα, αγ (or γα), γγ and αβ (or βα)[a]

	Donated hydrogens per molecule			
T/K	αα	αγ, γα	γγ	αβ, βα
394.9	1.3	1.3	1.0	1.5
319.4	1.7	1.7	1.2	1.9
261.9	1.9	1.9	1.4	2.0
197.3	2.1	2.2	1.5	2.7
119.6	2.3	2.4	1.5	2.7
39.9	2.4	2.5	1.5	2.8

[a] For χζ and ζχ conformers, the mean value is reported.

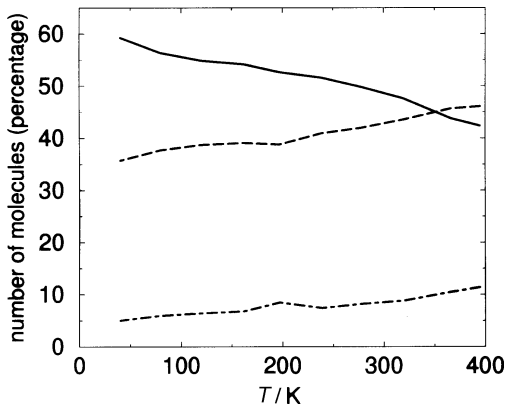

Fig. 4 Intra-molecular H-bond distribution. Percentage of molecules forming zero (———), one (– – – –) and two (— · —) intra-molecular H-bonds.

The average number of single H-bonds per molecule as well as of multiple H-bonds is shown as a function of temperature in Fig. 5. According to the convention adopted by Root and Berne,[21] an H-bond is defined as multiple when the hydrogen atom is involved in more than one inter-molecular H-bond or when the oxygen atom is involved in more than two inter-molecular H-bonds. At room temperature our values agree with those reported by Root and Berne.[21] Both curves of Fig. 5 show a clear inflection at the glass transition.

The average lifetime τ of an H-bond as a function of temperature is shown in Fig. 6. τ increases with decreasing temperature and diverges approaching the glass transition. The lifetime at room temperature is similar to that found in other H-bonded liquids. The inverse of the lifetime τ^{-1}, *i.e.* the number of H-bonds broken per unit time, can be fitted very accurately with an Arrhenius functional form (see inset in Fig. 6). The calculated value of the activation energy for the H-bond break is around 6.3 kJ mol^{-1}, comparable to the energy found in a computer simulation of liquid methanol.[34]

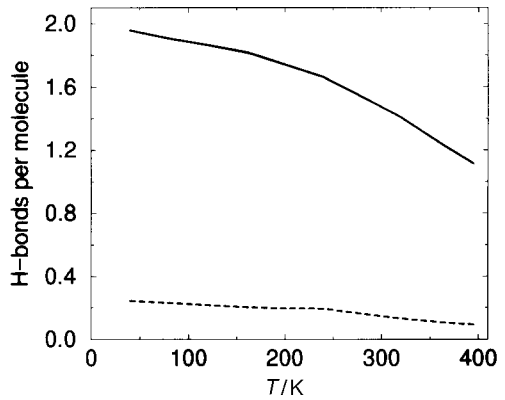

Fig. 5 Number of single (———) and multiple (—·—) inter-molecular H-bonds per molecule in liquid and glassy glycerol.

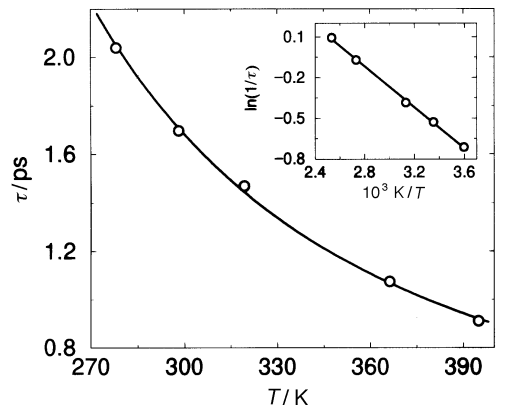

Fig. 6 Average lifetimes of the inter-molecular H-bond in liquid glycerol. The inset shows a fit of $\ln(1/\tau)$ *vs.* 10^3 K/T. The calculated lifetimes satisfy an Arrhenius law equation $1/\tau = A\exp[-B/(RT)]$ where $\ln(A) = 1.99 \pm 0.05$ and $B = 6.3 \pm 0.1$ kJ mol^{-1}.

3.2 Hydrogen bond network

Glycerol in its condensed phases is characterized by a high degree of association due to H-bonds. The viscosity[2] and the boiling point[15] in glycerol are unusually high; dielectric relaxation times are also extremely high in super-cooled glycerol[4] compared to other H-bonded liquids[36,37] and diverge near the glass transition.[5] The anomalous behaviour of the product of ion mobility and viscosity (Walden product) of KCl–glycerol solutions[4] has been ascribed to the existence of the H-bond network. Recently the existence of an H-bond network has also been invoked to explain the molecular reorientational mechanism investigated by nuclear magnetic resonance.[8] It is then of interest to investigate the extension of H-bond networks in liquid and glassy glycerol and to characterize their structural and dynamical properties.

At a given instant, two molecules are defined to be *connected* if at least one H-bond exists between them. Molecule A and molecule B belong to the same *hydrogen bond network* if one can go from A to B by crossing any number of connected molecules.

In the temperature range examined in the present study, glycerol tends to form *a single network* covering the entire sample. On average, 95% of molecules in the liquid at high temperature are connected. This network is very stable and, very seldomly, especially at high temperature, releases a few short living (less than 0.5 ps) monomers, dimers or trimers. In the glassy state, *only one* H-bonded network (100% of molecules) is observed throughout the sample during the entire simulation. The connectivity of the network can be further characterized by evaluating the average number of *connected* neighbors per molecule. In Table 4 we report the percentage fraction x_i of molecules belonging to the network as a function of the coordination number i ($i = 1, 2, \ldots, 8$) and of the temperature T. The mean coordination number, $N_c = \sum_{i=1}^{8} i x_i$, increases as the temperature decreases. In the glassy state, the H-bond network is frozen into a configuration where the average coordination number is about 4.6, larger than the coordination observed in the crystalline state, where each molecule has four neighbors.[16] Several molecules are found to be tetra- (30%) and penta-coordinated (43.4%) with a less important fraction of molecules with $i = 2$, 3, 6 and 7 and virtually none with $i = 1$ and 8.

With increasing temperature and beyond the glass transition, x_i shows a marked temperature dependence: highly coordinated molecules tend to disappear, whereas molecules bi- and tri-coordinated become more abundant. It is remarkable that the fraction x_4 is almost independent of temperature over the entire examined range.

Table 4 H-bond network connectivity[a]

T/K	x_1	x_2	x_3	x_4	x_5	x_6	x_7	x_8	N_c[b]
394.9	5.5	19.0	32.0	27.4	12.5	2.6	0.2	0.0	3.3
366.3	3.4	14.4	29.0	31.0	17.1	4.3	0.4	0.0	3.6
319.4	1.4	8.6	23.7	34.2	23.6	7.5	0.9	0.0	4.0
278.1	0.7	4.6	17.8	33.2	31.8	10.5	1.3	0.1	4.3
238.9	0.2	3.2	13.8	33.9	34.3	11.5	2.9	0.2	4.5
197.3	0.1	2.0	13.4	30.1	42.2	9.6	2.3	0.3	4.5
119.6	0.3	1.1	11.9	30.2	43.6	10.6	1.8	0.3	4.6
39.9	0.3	1.1	11.6	30.0	43.4	10.6	2.0	0.4	4.6

[a] x_i (with $i = 1, 2, \ldots, 8$) is the fraction of molecules belonging to the H-bond network and connected (see text) to i neighbors. [b] N_c is the mean coordination number.

To characterize the dynamical properties of the H-bond network, we define the following correlation function:

$$C(t) = \frac{\langle \boldsymbol{L}(t) \cdot \boldsymbol{L}(0) \rangle}{\langle \boldsymbol{L}(0) \cdot \boldsymbol{L}(0) \rangle} \quad (3)$$

where $\boldsymbol{L}(t)$ is a vector of length $N(N-1)/2$, N being the number of molecules in the sample. The generic element $L_k(t)$ refers to one pair of molecules, and is equal to one if the two molecules are connected at the time t, and zero otherwise. For a completely rigid structure the scalar product $\langle \boldsymbol{L}(t) \cdot \boldsymbol{L}(0) \rangle$ is equal, at any time, to the total number of connections in the network. The values of $C(t)$ at different temperatures for the liquid (400, 360 and 320 K), for the super-cooled liquid (280 and 240 K) and for the glass (200 K) are shown in Fig. 7. As previously stated, in the glassy phase, only a single configuration of the network is observed throughout the entire simulation and $C(t)$ does not decay. As extensively discussed in Part I,[1] the liquid was properly equilibrated and therefore the $C(t)$ function exhibits a temperature dependent decay giving quantitative information on the lifetime of the network. At temperatures near and below the freezing point the runs are too short to give reliable estimates of the characteristic time scale for the observed relaxation regimes. In the liquid state, on the contrary, the calculated $C(t)$ for a time run of 63 ps can be perfectly fitted using a superposition of three exponential decays. The three relaxation times t_1, t_2 and t_3 and the corresponding preexponential factors obtained from the fit of $C(t)$ at 400, 360 and 320 K are reported in Table 5, along with the corresponding χ^2 deviations. We infer therefore that the H-bond network breaks down through three distinct mechanisms, each with a characteristic time scale.

The faster mechanism is due to the vibrational motion of a molecule in the cage formed by its neighbors and is hence related to τ_E, the inverse of the Einstein frequency. The Einstein frequency can be estimated from the function

$$D(t) = \frac{1}{6t} \langle | \boldsymbol{R}(t) - \boldsymbol{R}(0) |^2 \rangle \quad (4)$$

where $\boldsymbol{R}(0)$ and $\boldsymbol{R}(t)$ are the vector position of a generic molecular center of mass at the zero time and at a later time t respectively, and the brackets indicate the average over the ensemble. At short times, $D(t)$ increases rapidly, reaches a maximum and, for $t \to \infty$, tends asymptotically to the translational diffusion coefficient[38] D_T. The position of the maximum of $D(t)$ gives an estimate of the inverse of the Einstein frequency. The calculated values of τ_E at 400, 360 and 320 K are reported in Table 5. Comparison with the values obtained for t_1 shows a reasonable agreement and the same trend with temperature. Due to the strengthening of H-bonds as the temperature is lowered, the Einstein frequency τ_E^{-1} is expected to increase correspondingly and thus τ_E to decrease.

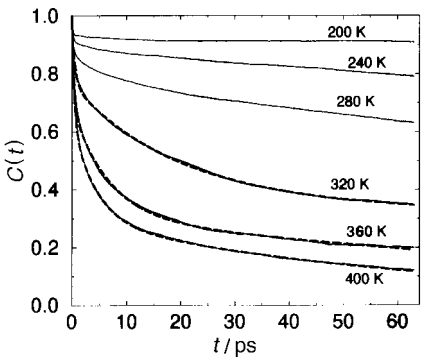

Fig. 7 Network connectivity correlation function as defined by eqn. (3) for liquid and glassy glycerol. Dashed lines are the results of the triexponential fit (see text).

The second mechanism for the breakdown of the H-bond network can be correlated to the time τ_C for neighbors to exchange in the cage. In order to estimate this time, we have computed the average time needed to replace all neighbors of a molecule. The values obtained for τ_C are given in Table 5 and agree almost quantitatively with the t_2 times.

The third and slowest mechanism for the breakdown of the H-bonded network is due to translational diffusion. The time τ_D, that a molecule takes to travel a distance d equal to the average distance between neighbors in the cage, corresponding to the peak in the center of mass pair distribution function, can be obtained from eqn. (4). For the calculation of τ_D we have computed the diffusion coefficients D_T and the distances d at 400, 360 and 320 K. The calculated values of D_T reported below are in good agreement with the experimental data of ref. 39.

$$D_T \simeq 6.99 \times 10^{-2} \text{ Å}^2 \text{ ps}^{-1} \quad \text{and} \quad d \simeq 5.4 \text{ Å at 400 K}$$

$$D_T \simeq 3.62 \times 10^{-2} \text{ Å}^2 \text{ ps}^{-1} \quad \text{and} \quad d \simeq 5.3 \text{ Å at 360 K}$$

$$D_T \simeq 1.14 \times 10^{-2} \text{ Å}^2 \text{ ps}^{-1} \quad \text{and} \quad d \simeq 5.2 \text{ Å at 320 K}$$

Using these data, we obtained for τ_D at 400 and 360 K a perfect agreement with the values of t_3 given in Table 5. At 320 K the agreement is less satisfactory, probably because the length of the run is not sufficient for a reliable estimate of τ_D and t_3. The time τ_E is even smaller in the glass with respect to the liquid and to the super-cooled liquid, due to the increase of the Einstein frequency as the cage becomes more rigid. In the super-cooled liquid the time scale τ_C for the cage breaking through neighbors exchanging is extremely slow while τ_D becomes virtually infinite. In the glass, also the neighbor exchange mechanism becomes too slow to be detected and τ_C is infinitely large.

4 Conclusions

The effects of inter-molecular interaction on the conformational distribution were investigated in a wide temperature range and for various phases at normal pressure. We found that in the gas phase in the range 300–400 K glycerol exhibits practically only three backbone conformations, namely αα, αγ and γγ. Inter-molecular interactions slightly stabilize the αα conformation and destabilize the γγ one as the temperature decreases. In the liquid near the freezing point, about half of the molecules are found in the αα conformation. The activation energy for a conformational transition was estimated from the temperature dependence of the number of conformational jumps in the unit time and was found to be around 20

Table 5 Parameters of the triexponential fit for the time decay of the H-bond network reported in Fig. 7[a]

T/K	A_1	t_1/ps	τ_E/ps	A_2	t_2/ps	τ_C/ps	A_3	t_3/ps	τ_D/ps	$\chi^{2\,b}$
394.9	0.35	0.43	0.34	0.34	4.3	3.5	0.29	69	69	8.68×10^{-6}
366.3	0.32	0.38	0.30	0.37	6.5	5.0	0.31	129	129	2.34×10^{-5}
319.4	0.20	0.32	0.25	0.39	18.3	11.0	0.38	489	395	1.45×10^{-5}

[a] Symbols are based on the expression $f(t) = A_1\ e^{-t/t_1} + A_2\ e^{-t/t_2} + A_3\ e^{-t/t_3}$. See text for details of τ_E, τ_C and τ_D. [b] χ^2 is the square of the standard deviation.

kJ mol^{-1}, *i.e.* much higher than RT at the freezing temperature. The high activation energy and the fact that nearly half of the molecules must undergo at least one conformational transition to reach the αα structure typical of the crystalline state are responsible for the remarkable stability of super-cooled glycerol.

The hydrogen bond structure and dynamics were also investigated. The average number of H-bonds per molecule ranges from about 2.1 in the glassy state to 1.2 in the liquid at high temperature. The average lifetime of the H-bond was found to be around 0.9 ps at 400 K and 2.0 ps in the supercooled liquid at 280 K. The temperature dependence of the inverse lifetime yielded an average activation energy of 6.3 kJ mol^{-1} to break the H-bond.

We found that a highly ramificated network of molecules connected through H-bonds exists in all phases and at all temperatures. The network dynamics, as probed by an appropriate correlation function, can be rationalized in terms of three distinct and increasingly longer time scales due to vibrational motion, to neighbor exchange and to translational diffusion.

Acknowledgements

This work was supported by the Italian Ministero dell'Università e della Ricerca Scientifica e Tecnologica (MURST), by the Consiglio Nazionale delle Ricerche (CNR) and by the European Union (contract No. ERBFMGECT950017). We thank Massimo Marchi for providing the new version of the ORAC program[40] and Raffaele Della Valle for valuable suggestions.

References

1 R. Chelli, P. Procacci, G. Cardini, R. G. Della Valle and S. Califano, *Phys. Chem. Chem. Phys.*, 1999, **1**, 871.
2 D. B. Davies, A. J. Matheson and G. M. Glover, *J. Chem. Soc., Faraday Trans. 2*, 1973, **69**, 305.
3 R. L. Cook, H. E. King Jr., C. A. Herbst and D. R. Herschbach, *J. Chem. Phys.*, 1994, **100**, 5178.
4 D. C. Champeney and F. O. Kaddour, *Mol. Phys.*, 1984, **52**, 509.
5 N. Menon and S. R. Nagel, *Phys. Rev. Lett.*, 1995, **74**, 1230.
6 D. C. Champeney, R. N. Joarder and J. C. Dore, *Mol. Phys.*, 1986, **58**, 337.
7 M. Garawi, J. C. Dore and D. C. Champeney, *Mol. Phys.*, 1987, **62**, 475.
8 R. Böhmer and G. Hinze, *J. Chem. Phys.*, 1998, **109**, 241.
9 M. R. Carpenter, D. B. Davies and A. J. Matheson, *J. Chem. Phys.*, 1967, **46**, 2451.
10 N. Menon and S. R. Nagel, *Phys. Rev. Lett.*, 1995, **74**, 1230.
11 M. Rajeswari and A. K. Raychaudhuri, *Phys. Rev. B*, 1993, **47**, 3036.
12 Y. H. Jeong, S. R. Nagel and S. Bhattacharya, *Phys. Rev. A*, 1986, **34**, 602.
13 W. T. Grubbs and R. A. MacPhail, *J. Chem. Phys.*, 1994, **100**, 2561.
14 S. Kojima, *Phys. Rev. B*, 1993, **47**, 2924.
15 *Handbook of Chemistry and Physics*, ed. D. R. Lide, CRC Press, Boca Raton, 78th edition, 1997–1998.
16 H. van Koningsveld, *Rec. Trav. Chim.*, 1968, **87**, 243.
17 A. V. Hook, *Crystallization Theory and Practice*, Reinhold Press, New York, 1961.
18 O. Bastiansen, *Acta Chem. Scand.*, 1949, **3**, 415.
19 J. Dawidowski, F. J. Bermejo, R. Fayos, R. Fernández-Perea, S. M. Bennington and A. Criado, *Phys. Rev. E*, 1996, **53**, 5079.
20 L. J. Root and F. H. Stillinger, *J. Chem. Phys.*, 1989, **90**, 1200.
21 L. J. Root and B. J. Berne, *J. Chem. Phys.*, 1997, **107**, 4350.
22 P. F. Blackmore, J. F. Williams and M. G. Clark, *J. Chem. Educ.*, 1973, **50**, 55.
23 R. W. Swick and A. Nakao, *J. Biol. Chem.*, 1954, **206**, 883.
24 P. Schambye, H. G. Wood and G. Popjak, *J. Biol. Chem.*, 1954, **206**, 875.
25 L. I. Gidez and M. L. Karnovski, *J. Am. Chem. Soc.*, 1952, **74**, 2413.
26 M. Gibbs, R. Dumrose, F. A. Bennett and M. R. Bulbeck, *J. Biol. Chem.*, 1950, **184**, 545.
27 A. L. Lehninger, *Principles of Biochemistry*, Worth, New York, 1982.
28 B. J. Teppen, M. Cao, R. F. Frey, C. van Alsenoy, D. M. Miller and L. Schäfer, *J. Mol. Struct. (THEOCHEM)*, 1994, **314**, 169.
29 L. van Den Enden, C. van Alsenoy, J. N. Scarsdale and L. Schäfer, *J. Mol. Struct. (THEOCHEM)*, 1983, **104**, 471.
30 C. van Alsenoy, *J. Mol. Struct. (THEOCHEM)*, 1985, **121**, 153.
31 W. H. Press, B. P. Flannery, S. A. Teukolsky and W. T. Vetterling, *Numerical Recipes*. Cambridge University Press, London, 1987.
32 G. M. Torrie and J. P. Valleau, *J. Comput. Phys.*, 1977, **23**, 187.
33 M. Soltwisch and B. Steffen, *Z. Naturforsch. A: Phys. Sci.*, 1981, **36**, 1045.
34 P. Sindzingre and M. L. Klein, *J. Chem. Phys.*, 1992, **96**, 4681.
35 M. Haughney, M. Ferrario and I. R. McDonald, *J. Chem. Phys.*, 1987, **91**, 4934.
36 U. Kaatze and V. Uhlendorf, *Z. Phys. Chem. N. F.*, 1981, **126**, 151.
37 D. Bertolini, M. Cassettari and G. Salvetti, *J. Chem. Phys.*, 1982, **76**, 3285.
38 M. P. Allen and D. J. Tildesley, *Computer Simulation of Liquids*, Clarendon Press, Oxford, 1987.
39 D. J. Tomlinson, *Mol. Phys.*, 1972, **25**, 735.
40 P. Procacci, T. A. Darden, E. Paci and M. Marchi, *J. Comput. Chem.*, 1997, **18**, 1848.

Paper 8/08957D